Hints on the lateralization of dopamine binding to D_1 receptors in rat striatum

Rafael Franco*[1,2], Verònica Casadó-Anguera[1,2], Ana Muñoz[1,3], Milos Petrovic[4,5], Gemma Navarro[1,2], Estefanía Moreno[1,2], Jose Luís Lanciego[1,5], José Luis Labandeira-Garcia[1,3], Antoni Cortés[1,2], Vicent Casadó[1,2]

[1] CIBERNED. Centro de Investigación Biomédica en Red sobre Enfermedades Neurodegenerativas. Instituto de Salud Carlos III. Valderrebollo 5. 28031 Madrid. Spain.

[2] Molecular Neurobiology Laboratory. Department of Biochemistry and Molecular Biology. Faculty of Biology. University of Barcelona. 28028 Barcelona. Spain.

[3] Laboratory of Neuroanatomy and Experimental Neurology. CIMUS (Center for Research in Molecular Medicine and Chronic Diseases). University of Santiago de Compostela. 15782 Santiago de Compostela, Spain.

[4] School of Pharmacy and Biomedical Sciences, University of Central Lancashire, PR1 2HE, Preston, UK.

[5] Institute of Physiology, Academy of Sciences, Videnska 1083, 14220 Prague, Czech Republic.

[5] Laboratory of Neuroanatomy of Basal Ganglia, Neurosciences Division, Center for Applied Medical Research (CIMA), University of Navarra, 31008 Pamplona, Spain.

* Corresponding author:
Rafael Franco
Dept. of Biochemistry and Molecular Biology
Faculty of Biology. University of Barcelona
Diagonal 645. Prevosti Building
08028 Barcelona. Spain.
rfranco@ub.edu
+34 934021208

Abstract

Dopamine receptors in striatum are important for healthy brain functioning and are the target of levodopa-based therapy in Parkinson's disease. Lateralization of dopaminergic neurotransmission in striata from different hemispheres occurs in patients, but also in healthy individuals. Our data show that the affinity of dopamine binding to dopamine D_1 receptors is significantly higher in left than in right striatum. Analysis of data from radioligand binding to striatal samples from naïve, 6-hydroxydopamine lesioned, levodopa-treated and levodopa-induced dyskinetic rats shows differential receptor structure and gives hints on the causes of right/left lateralization of dopamine binding to striatal D_1 receptors. Moreover, binding data showed loss of lateralization in levodopa (L-DOPA)-induced dyskinetic rats.

Running title: Lateralization of binding to striatal dopamine D_1 receptors

Keywords: lateralization, basal ganglia, G protein coupled receptor dimer, dyskinesia, 6-hydroxydopamine, cooperativity index.

Introduction

Motoric lateralization is due to musculoskeletal and brain asymmetries and does occur in both vertebrates and invertebrates (see [1] for review). In mammalian brain, asymmetries have been mainly studied from an anatomic point of view. Thus, early but accurate studies in human entorhinal area showed right-left asymmetry in the number of neurons [2]. Assessment of lateralization at the molecular level was approached by radioligand binding studies mainly assuming similar receptor species in both hemispheres and reporting differences in receptor expression. For instance, dopamine D_1 receptor lateralization and correlation of dopamine D_1/D_2 receptor expression ratio with apomorphine-induced rotation was assessed by differences in Bmax, *i.e.* in differences in the amount of receptors ([3] and references therein). Despite enormous conceptual interests, the lack of suitable tools is delaying the increase in knowledge of the molecular causes of brain asymmetry. Recent discoveries indicate that dopamine receptors, as members of the G-protein-coupled receptor (GPCR) superfamily, interact with a variety of proteins [4] and that the quaternary structure affects GPCR binding characteristics and signaling [5]. Differences in the affinity of neurotransmitters/neuromodulators binding to specific receptors have served to detect molecular differences in pre- versus post-synaptic GPCRs [6]. These findings open a way to hypothesize that lateralization in mammalian brain may be addressed by careful study of the affinity of agonist binding to receptors in the two hemispheres.

Dopaminergic neurotransmission in the striatum has a key role in motor control. Thus, the lack of nigrostriatal dopaminergic innervation in Parkinson's disease results in motor alterations. Previously published data have clearly established that left and right striatum are not the same: apparent asymmetry between neurochemical properties of striata from opposing hemispheres exists [7] and, unsurprisingly, the same applies to dopaminergic neurotransmission [8]. This lateralization in the striatum at the circuit and the cellular levels has both behavioral consequences [9] and therapeutic implications in PD therapy [10]. For example, lateralization in $D_{2/3}$ receptor binding was i) found in response to unpredictable reward and could be accounted for by sex differences [11],ii) associated with motor activity [12], iii) correlated to the body-mass index (BMI) of non-obese males [13], iv) found to predict individual differences in learning from reward versus punishment, thus underlying human personality and cognition [14] and v) found to correlate with incentive motivation, with greater positive incentive motivation being associated with higher receptor availability

in the left hemisphere [15]. However, the molecular dissection of such asymmetry is still lacking [16]. Recently, we have reported left vs. right asymmetry of dopamine binding to rat striatal dopamine D_1 receptors (D_1Rs) indicating that the dopamine-mediated signaling has a stronger tone in the left hemisphere [17]. This lateralization, consistently found in samples from healthy rats, is not due to right-left limb preferences and, therefore, it may likely be a property crucial for proper motor control in mammals. The aim of this paper was to look for hints to understand the molecular basis of lateralization of dopamine binding in right and left striatum.

Methods

8-week old male Wistar rats were used in the experiments. All experiments were carried out in accordance with the "Principles of laboratory animal care" and approved by the corresponding committee at the University of Santiago de Compostela, Spain. After anesthesia with ketamine/xylazine (1 % ketamine, 75 mg/kg; 2 % xylazine, 10 mg/kg), and placement in a David Kopf stereotaxic apparatus, animals received a unilateral injection in the right medial forebrain bundle of 12 μg of 6-OHDA HBr Sigma; prepared in 4 μL of sterile saline containing 0.2 % ascorbic acid. The stereotaxic coordinates were 3.7 mm posterior to bregma, −1.6 mm lateral to midline, and 8.8 mm ventral to the skull at the midline, in the flat skull position. The solution was injected with a 5-μL Hamilton syringe coupled with a motorized injector (Stoelting,Wood Dale, Il, USA) at 1 μL/min, and the cannula was left in situ for 2 min after injection. Three weeks later, the efficacy of the lesion was evaluated by the amphetamine rotation and the cylinder test. The correct nigrostriatal lesion was confirmed by the loss of tyrosine hydroxylase (TH) immunohistochemistry staining.

Animals were divided into four groups as follows: 1) non-lesioned rats (naïve); 2) animals lesioned by 6-hydroxydopamine (6-OHDA), but receiving only vehicle afterwards (lesioned); 3) animals lesioned by 6-OHDA receiving a chronic treatment with levodopa (L-DOPA), 6mg/kg plus 10 mg/kg of benserazide daily for 3 weeks without exhibiting adverse motoric reactions (L-DOPA treated non-dyskinetic) and 4) same as 3), but showing adverse motoric reactions (L-DOPA treated dyskinetic). Benserazide is a peripheral decarboxylase inhibitor that increases brain availability of L-DOPA. The development of dyskinesia was tested using the rodent abnormal movement scale (AIMs) [18]. For binding studies, animals were sacrificed by decapitation (6 h after the last injection of vehicle or L-DOPA), and the brains

were removed rapidly. Brain areas containing the striatum (both from the lesioned and intact hemispheres) were dissected out and immediately frozen on dry ice until use. A more detailed description of procedures may be found in Farré et al. [17], which also describes the radioligand binding protocols. In brief, membrane suspensions were preincubated in 50 mM Tris-HCl buffer, pH 7.4, containing 10 mM $MgCl_2$ with 1 nM of radiolabelled D_1R antagonist [^{3}H]R-(+)-7-chloro-8-hydroxy-3-methyl-1-phenyl-2,3,4,5-tetra-hydro-1H-3-benzazepine ([^{3}H]SCH 23390), and increasing concentrations of (±)-1-phenyl-2,3,4,5-tetrahydro-(1H)-3-benzazepine-7,8-diol hydrobromide (SKF 38393, D_1R agonist, triplicates of 15 different competitor concentrations from 0.01 nM to 50 μM), in the absence or the presence of 100 nM of the D_3 receptor agonist trans-7-hydroxy-2-[N-propyl-N-(3'-iodo-2'-propenyl)amino]tetralin (7-OH-PIPAT). Nonspecific binding was determined in the presence of 50 μM SCH 23390.

Radioligand competition curves were analyzed by nonlinear regression using the commercial Grafit curve-fitting software (Erithacus Software, Surrey, UK). Two different models were used for data analysis, one assuming receptor monomers and another assuming receptor dimers. First of all, the equations of the classical two-independent site model were used; the model assumes receptors in two affinity states: low affinity/not coupled to G proteins and high affinity/G-protein-coupled. Second, equations of the two-state dimer receptor model were used [19, 20]. In the latter, a homodimer is considered the minimal structural unit of a receptor forming homomers or forming heteromers with another receptor. To calculate the macroscopic equilibrium dissociation constants [21], data from competition binding experiments were fitted using the following equation:

$$A_{\text{total bound}} = (K_{DA2}A + 2A^2 + K_{DA2}AB / K_{DAB})\, R_T / (K_{DA1}K_{DA2} + K_{DA2}A + A^2 +$$

$$K_{DA2}\, AB/ K_{DAB} + K_{DA1}K_{DA2}B /K_{DB1} + K_{DA1}K_{DA2}B^2 / (K_{DB1}K_{DB2})) + A_{\text{non-specific bound}} \quad \text{Eq. 1}$$

where A represents free radioligand (the D_1 partial agonist [^{3}H]SCH 23390) concentration, R_T is the total amount of receptor dimers and K_{DA1} and K_{DA2} are the macroscopic equilibrium dissociation constants describing the binding of the first and the second radioligand molecule (A) to the dimeric receptor; B represents the assayed competing compound (SKF 38393) concentration, and K_{DB1} and K_{DB2} are, respectively, the macroscopic equilibrium dissociation constants for the binding of the first competitor molecule (B) to an unoccupied dimer and for

the binding of the second competitor molecule (B) to the semi-occupied dimer; K_{DAB} is the hybrid equilibrium radioligand/competitor dissociation constant, which is the dissociation constant of B binding to a receptor dimer semi-occupied by A.

As the radioligand A ([^{3}H] SCH 23390) shows non-cooperative behavior, determining K_{DA1} is sufficient to characterize the binding of the radioligand, A, and Eq. (1) leads to Eq. (2) by establishing $K_{DA2} = 4K_{DA1}$ [19, 20]:

$$A_{total\ bound} = (4K_{DA1}A + 2A^2 + 4K_{DA1}AB / K_{DAB})\ R_T / (4K_{DA1}^2 + 4K_{DA1}A + A^2 + 4K_{DA1}AB / K_{DAB} + 4K_{DA1}^2B / K_{DB1} + 4K_{DA1}^2B^2 / (K_{DB1}K_{DB2})) + A_{non\text{-}specific\ bound} \quad \text{Eq. 2}$$

The concentration of competitor B that leads to a 50% of binding sites occupied by the competitor B molecule is the B_{50} value. Assuming two independent sites, we have devised the equation 3 to obtain B_{50} from calculated parameters, using the equation corresponding to the two-independent site model (full deduction of Eq. 3 is available upon request)

$$B_{50} = [(B_{maxH} - B_{maxL})\ (K_{DH} - K_{DBL}) + ((B_{maxH} - B_{maxL})^2\ (K_{DH} - K_{DBL})^2 + 4B_{max}^2K_{DH}K_{DBL})^{1/2}] / 2B_{max} \quad \text{Eq. 3}$$

where B_{max} represents the maximum binding to high plus low affinity sites: $B_{max} = B_{maxH} + B_{maxL}$).

In the case of receptor dimers, the B_{50} value is readily calculated [20] by the following formula:

$$B_{50} = (K_{DB1}K_{DB2})^{1/2} \quad \text{Eq. 4}$$

Goodness of fit was tested according to reduced chi-squared values given by the Grafit program. The test of significance for two different model population variances was based upon the F distribution (see [19, 22] for details). Using this F test, a probability greater than 95% ($p < 0.05$) was considered the criterion to select a more complex model (i.e. Eq. (1) or two-sites in the two-independent site model) over the more simple one (i.e. Eq. (2) or one site in the two-independent site model). Competition curves for each animal were performed in triplicates to obtain accurate parameter values (see [17]). Differences were analyzed for significance by two-way ANOVA followed by Bonferroni's post hoc multiple comparison tests.

Results

Binding to dopamine D_1Rs in right and left rat striatal membranes was performed using [^{3}H]SCH 23390, a D_1R antagonist, and SKF38393, a D_1R agonist, as competitor, in the presence or absence of a dopamine D_3 receptor agonist (7-OH-PIPAT) (see [17]). The data from the competition curves were fitted using equations devised from two models: the two-independent site model and the two-state dimer model.

Fitting data using the two-independent site paradigm

The two-independent site model assumes that high- and low-affinity binding is due to, respectively, GPCRs coupled and uncoupled to a given heterotrimeric G protein. Data from competition assays analyzed using this model provide equilibrium constants for high- (K_{DH}) and for low-affinity (K_{DL}) binding, as well as for the amount of high and low affinity sites (Table 1). According to the *two-independent site* model, two D_1R binding species are distinguishable in striatal samples from either hemisphere of naïve rats. Lateralization is observed by the statistically significant lower K_{DH} and K_{DL}–values in the left hemisphere compared with values in the right one: K_{DH} is 14-fold lower and K_{DL} is circa-3-fold lower in the left striatum. In addition, the proportion of high affinity sites is 3-fold lower in the left hemisphere.

Low affinity species were predominant in hemilesioned animals in which, interestingly, the affinity parameters (K_{DH} or K_{DL}) for the binding of the agonist to D_1Rs were similar in the striata from two sides (Table 1). Taking into account all four groups of animals, the overall comparison showed that the proportion of high-affinity (B_{maxH}) vs. total number of sites was significantly different (inter-group differences detected by two-way ANOVA) in samples from both right ($F_{(3,16)}$=7.79, p=0.002) and left ($F_{(3,16)}$=12.80, p=0.0002) hemispheres. Right-left lateralization was also found in terms of differential (inter-hemisphere differences detected by two-way ANOVA) B_{maxH} ($F_{(1,16)}$=30.5, p<0.0001), K_{DH} ($F_{(1,16)}$=91.0, p<0.0001) and K_{DL} ($F_{(1,16)}$=43.1, p<0.0001) values (see Table 1). Interpretation of results in terms of D_1Rs coupled and uncoupled to G proteins is complex. In principle, the preponderance of low affinity sites (Table 1) indicates that G-protein-coupled D_1Rs would be the minority species in all samples except in the right striatum of naïve and dyskinetic animals.

In contrast to the results for B_{maxH}, the values for B_{50} (i.e. the concentration of SKF38393 that leads to a 50% of binding sites occupied by this agonist), calculated using the two-site model-derived Eq. 3, were similar in the two hemispheres and were also similar in samples from the different groups. However, there are inter-group differences if B_{50} values are calculated under the dimer paradigm (see later).

Fitting data using the two-state dimer receptor paradigm

The binding to dimers is determined by the total number of dimers (maximum number of binding sites B_{max} would be twice the number of dimers R_T) and two equilibrium constants defining the binding of the competing agonist (B) to the two protomers of the dimer (K_{DB1} and K_{DB2}). If agonist binding to the first protomer in an unoccupied dimer modifies the characteristics of the binding to the second protomer, cooperativity occurs and a homotropic cooperativity index (D_{CB}) may be readily calculated. Apart from higher affinity in the left hemisphere in samples from all animal groups, the cooperativity index is more negative in the left hemisphere (Table 2). Thus, data fitting using equations devised from the dimer receptor model shows right/left lateralization.

Interestingly, the data fit under the dimer paradigm allows calculation of a hybrid constant that quantifies the modulation due to the binding of another ligand to the partner receptor in a dimer. The hybrid parameter (D_{AB}) denotes whether the binding of the competitor (B) to unoccupied receptors and to receptors hemioccupied by the radioligand (A) is similar or not. Deviations from zero values for D_{AB} indicate that binding of the radioligand molecule to one protomer affects the binding of the competitor to the second protomer in the dimer. Importantly, D_{AB} was always zero in samples from right striatum, but not in those from left striatum (Table 2), *i.e.* two-way ANOVA analysis showed significant inter-hemispheric differences in K_{DAB} ($F_{(1,16)}$=324.6, p<0.0001). Although differences in values were detected in the left striatum of every experimental group, the D_{AB} was always positive, thus indicating that the binding of the competitor to the left striatal D_1Rs is favored if one molecule of the radioligand is already bound to the receptor dimer. Non-zero D_{AB} values were confirmed by comparing the goodness of the fit with and without considering interactions due to A affecting the binding of B to the dimer. In fact, the fitting was significantly better when D_{AB} was parameterized than when D_{AB} was forced to be zero. Furthermore, the robustness of the overall results from all conditions and from the two hemispheres was higher when the

parameter was taken into account. These results indicate the convenience of considering the D_{AB} hybrid parameter under the receptor dimer concept.

The B_{50} values obtained under the dimer receptor paradigm (see Eq. 4) confirm lateralization, with lower values in the left hemisphere (significant inter-hemispheric differences in B_{50} by two-way ANOVA analysis ($F_{(1,16)}$=233.9, p<0.0001), and with no major alterations in samples from lesioned animals (with respect to the samples from naïve rats, see Table 2). Therefore, B_{50} may better reflect agonist-binding characteristics if calculated under the receptor dimer assumption, *i.e.* using eq. 4.

Hints on lateralization of binding to D_1Rs in naïve animals

Lateralization of dopamine binding to D_1Rs in striatum reflects changes in the molecular structure of the binding site that may be due to several circumstances. The different possibilities may be summarized as different degree of coupling of D_1R to other molecules of D_1R itself or to other proteins (see Discussion for D_1R-interacting proteins). It should be noted that the use of isolated membranes simplifies the interpretation of the results as in membranes the two more likely types of interactions are the homo/heteromeric with GPCRs and the coupling to G proteins. The data from samples of naïve animals using the two-independent site model may be interpreted as more D_1Rs coupled to G proteins in the right side. The proportion of high (18%) and low (82%) affinity sites in the left side (Fig. 1) points to a marked imbalance in the left hemisphere where receptors seem to be less coupled to heterotrimeric G proteins. The K_{DH} and K_{DL} values, both of which were significantly lower in the left hemisphere (Table 1) indicate that, irrespective of G protein coupling, the D_1R in the left hemisphere is structurally different from the D_1R in the right hemisphere. Either this is due to the coupling to a different G protein or reflects allosteric effects due to membrane components other than G proteins. Although D_1Rs may couple to Gq and lead to calcium mobilization via D_1-D_2 receptor heteromer formation ([23, 24]) and other less well defined mechanisms [25], the main signaling pathway engaged via striatal D_1Rs seems to be Gs-dependent [26, 27].

The existence of allosteric effectors differentially affecting the binding to D_1R in the two striatal hemispheres is confirmed by results obtained using the two-state dimer receptor model. First of all, negative cooperativity is more marked in the left side (Table 2). From the analysis using the dimer receptor model, a relevant result comes out: there is a lack of

heterotropic agonist/antagonist effect in the binding to D_1Rs on the right side, whereas the heterotropic agonist/antagonist effect in the binding exists on the left side. In fact, D_{AB} is zero in data from the right side and >0 in data from the left side. Main structural differences in the D_1R from right and left sides occur as only the binding of the radiolabelled antagonist to the left D_1R affects the binding of competing agonist. Hence, the D_1R in the left striatum changes its conformation when occupied with the radioligand in such a way that the access of the competitor to a hemioccupied receptor is better than to the empty dimer (Table 2). The underlying mechanisms are difficult to apprehend, but this piece of evidence is in itself very relevant because it allows distinguishing between two qualitatively different D_1R subpopulations. As the binding to the right hemisphere does not display the heterotropic agonist/antagonist effect, the observed lateralization is due to structurally different D_1Rs. Furthermore, the positive effect contrasts with the negative cooperativity found often in agonist binding to GPCRs [19, 28]. In terms of dimers, the results indicate that the access of the second radiolabelled molecule to D_1R dimers is thermodynamically less favored, whereas the opposite occurs when the competitor binds to the dimer already occupied by one radiolabelled molecule. In summary, according to the two-independent site model, in the left hemisphere, the fraction of D_1Rs coupled to G proteins is lower than the fraction of uncoupled ones. Under the receptor dimer assumption, an allosteric effect may explain why D_1Rs in the left side display higher affinity. Also, the dimer model-devised parameter D_{AB} seems to be a convenient way to describe intradimer interactions.

Hints on lateralization of binding to D_1R in lesioned and dyskinetic animals

According to the two-independent site model, the balance of high (B_{maxH}) and low (B_{maxL}) affinity sites does not change much in the left hemisphere of lesioned animals or of lesioned animals treated with L-DOPA, but the B_{maxH}/B_{maxL} ratio is markedly reduced in the right striatum. Remarkably, the K_{DH} and K_{DL} values are markedly reduced in the right side, thus indicating a higher affinity of the agonist binding to D_1R in lesioned animals (with or without L-DOPA treatment) than in naïve animals (Table 1).

Comparing the data from lesioned and naïve animals, the use of the dimer receptor model provided K_D (K_{DB1} or K_{DB2}) values that were similar in the right and in the left hemispheres. Similarly, there was no statistical differences in the values of the cooperativity index (D_{CB}) and of the D_{AB} and K_{DAB} parameters between animal groups or between left and right sides. In contrast to the two-independent site model, K_{DB1} and K_{DB2} values showed similar

lateralization in lesioned and naïve animals (Table 2); two-way ANOVA analysis showed significant inter-hemisphere differences in K_{DB1} ($F_{(1,16)}$=237.2, p<0.0001) and K_{DB2} ($F_{(1,16)}$=204.4, p<0.0001). The dimer receptor model confirms the similar binding to D_1Rs in the right side in naïve and dyskinetic animals. In summary, in animals from all treated groups, the dimer assumption model robustly keeps the binding characteristics (lateralization included) found in naïve animals.

According to the two-independent site model, dyskinesia totally eliminates the high/low affinity imbalance in the right striatum of lesioned (plus/minus L-DOPA) animals; in fact, the percentage of high affinity sites in the right side of dyskinetic animals is 57% (58% in naïve animals) and the K_{DH} is 24 nM (28 nM in naïve animals). The dopamine binding to D_1Rs in the left side of dyskinetic animals is more similar to that in naïve animals, but the proportion of high affinity sites is higher than in any other group (33% versus 12-22%).

Impact of agonist binding to D_3 receptors on lateralization of binding to D_1R

In samples from all groups except the dyskinetic one, the effect of the D_3 receptor agonist, 7-OH-PIPAT, was monotonous, *i.e.* it did not affect in a qualitative manner the lateralization in terms of K_D values of agonist binding to striatal D_1R. In dyskinetic animals, the treatment with the D_3 receptor agonist led to the disappearance of such lateralization. In fact, using the two-independent site model, K_{DH} values became similar in both hemispheres in dyskinetic animals (also in lesioned animals) (Table 1). Using the receptor dimer paradigm, K_{DB1}, K_{DB2} or cooperativity index (D_{CB}) values were similar in the right and left striatum of dyskinetic animals (Table 2). Quite noteworthy was that the activation of the D_3R led to the appearance of the heterotropic D_1R agonist/antagonist effect in the right side of dyskinetic, but not of naïve or lesioned (plus/minus L-DOPA) rats. Furthermore, the B_{50}, calculated according to the dimer receptor model, is reduced in the right striatum to become similar to that in the left striatum. In contrast, B_{50} values calculated according to the two-independent site model are monotonously high irrespective of the animal group, of the hemisphere and of treatment (or not) with the D_3 receptor agonist. Comparison of the data in the absence and the presence of the D_3R agonist confirms lateralization and suggests that parameters obtained using the dimer model are more robust (than using the two-independent-site model) to explain and interpret radioligand binding results.

Discussion

More than 3 decades ago, Yamamoto et al. [29] reported striatal lateralization of dopamine release in animals under a motor task related to sucrose/water reward. Lateralization of dopamine release mechanisms may run in parallel with lateralization of the dopamine receptor signaling system. In fact, PET assays using a D_1R ligand [^{11}C]NNC-112 show asymmetry across hemispheres in healthy humans [30], thus pointing towards differential dopamine-mediated signaling mechanisms in right and left striatum. This lateralization occurring at the very molecular level adds further complexity in the neural circuits operating in the most important region for motor control. Elucidation of the causes and consequences of lateralization in dopamine binding and dopamine-receptor-mediated signaling is key to understand the role of striatal asymmetry in motor control and to design better interventions to prevent and/or manage PD.

Back in the third quarter of the twentieth century, radioligand binding techniques were instrumental to identify receptors for neurotransmitters. Autoradiography was also instrumental to make the first maps of receptor expression in the CNS. Last but not least, fitting radioligand binding data was key to determine the affinity of the transmitter-receptor interaction. More recently, the technique has been mainly used to determine differences of receptor expression in neuropathologies. In Parkinson's disease, alterations in the levels of striatal dopamine receptors have been reported [31-34]. Often, the results of the comparison assays are attributed to differences in the levels of expression and not to qualitative changes in the characteristics of the binding. Experiments using a single concentration of the radioligand (even in competition assays) cannot provide unequivocal data on the actual levels of receptors. An alteration in specific binding using a single concentration of the radioligand may be due to actual differences in receptor levels or to differential binding characteristics in receptors from the two samples being compared. A proper assessment of receptor levels and ligand-receptor affinity needs optimal experimental design and careful analysis of the data. Indeed, radioligand binding appears as instrumental to detect differential trends in the molecular characteristics of receptors.

The information provided by fitting the data to two-independent site and to two-state dimer receptor models is summarized in Tables 1 and 2 and in Fig. 1. D_1Rs in the left striatum have higher affinity for agonists than in the right striatum and this seems to be due to a higher percentage of receptors coupled to G proteins. The potential heteromerization with D_3Rs does

not play any role in lateralization found in naïve and lesioned rats (see below for discussion of data from dyskinetic animals). The homotropic effect, *i.e.* that exerted by one compound upon the previous binding of the same compound, may be either due to cooperativity in the binding to a receptor dimer or to the occurrence of G-protein-coupled high- and G-protein-uncoupled low-affinity monomers. The binding properties within the left striatum also showed a heterotropic effect, *i.e.* an effect of the binding of the radiolabelled antagonist on the binding of the competing agonist. Occurrence of receptors dimers in which the binding of the radioligand to a protomer in the dimer affects the binding of the competitor to the second protomer in the dimer is a reasonable hypothesis to explain the heterotropic agonist/antagonist effect. In summary, our conclusion is that the left striatum displays a D_1R with a tertiary and/or quaternary structure different from that in the right side. Different quaternary structure may be due to a different stoichiometry of the receptor (monomer versus dimer) and/or may be the consequence of allosteric modulation due to differential coupling to G or other proteins, including other GPCRs. Actually, the couple formed by D_1 and adenosine A_1 receptors is recognized as the first identified GPCR heteromer formed by two different receptor types [35, 36]. Heteromerization and allosteric modulation affect the quaternary structure of GPCRs and, therefore, they often affect the affinity of the radioligand/GPCR interaction [5, 37-40]. D_1R may form heteromers with other GPCRs (see: www.iiia.csic.es/~ismel/GPCR-Nets/ and [41]) and it may also interact with proteins such as NMDA glutamate ionotropic receptors [42-45], N-type calcium channels [46] and calcyon [47].

Coexpression of D_1Rs and calcyon in heterologous systems decreases the proportion of high/low affinity D_1R sites [48]. As calcyon is elevated in patients with schizophrenia [47], it is likely that the reported decrease in the proportion of D_1R in the disease detected by autoradiography [49] comes from a decrease of high-affinity sites rather than by a decrease in the total amount of receptors. In the 6-hydroxydopamine-hemilesioned rat model of Parkinson's disease, the total amount of D_1Rs does not significantly change ([17] and Table 1 and 2). In contrast, the characteristics of the binding (high/low affinity ratio using the two-independent site model or cooperativity using the dimer receptor model) in samples from lesioned animals were different (Table 1 and 2 and Fig. 1). Interestingly, the affinity constants and total receptor amounts were similar in right and left striata from naïve and dyskinetic animals. However, in samples from dyskinetic animals, there was a differential trend, namely the appearance of the heterotropic D_1R agonist/antagonist effect in the right

striatum, but only when the D_3R agonist, 7-OH-PIPAT, was present in the assays. The increase in D_3R expression in dyskinesia leads to a marked D_1-D_3 heteromerization in striatum [17]. The appearance of the peculiar and not previously detected heterotropic agonist/antagonist effect may be due to alterations in the quaternary structure of the D_1R due to activation of D_3R interacting with D_1Rs. L-DOPA therapy results in markedly high concentrations of dopamine in the CNS; consequently, D_3Rs are likely activated under a L-DOPA administration regime such as that used in Parkinson's disease patients. Taken together, the results indicate that a high dopaminergic tone in dyskinetic animals makes D_1Rs similar in right and left striatum. Moreover, the lateralization in dopamine binding to striatal D_1Rs, shown in naïve, lesioned and non-dyskinetic animals, was virtually absent in the dyskinetic state. Abnormal movements in dyskinetic animals may be due to the loss of this D_1R lateralization.

Further experimental effort would be necessary to establish the reasons why dopamine binding to striatal D_1R is lateralized. Differential D_1R structure in right versus left sides may come as a result of interactions with other membrane proteins or with interactions with different scaffolding or G proteins (Fig. 2).

Acknowledgments

This work was supported by grants from Spanish *Ministerio de Ciencia y Tecnología* [SAF2009-07276, SAF2011-23813 and SAF2012-39875-C02-01] and from Spanish *Ministerio de Salud* [PI09/01756]. MMP is supported by Marie Curie CIG PCIG11-GA-2012-322013.

Conflict of interest

The authors declare no conflict of interest.

References

1. Frasnelli, E., *Brain and behavioural lateralization in invertebrates.* Frontiers in Psychology, 2013. **4**.
2. Heinsen, H., R. Henn, W. Eisenmenger, M. Gotz, J. Bohl, B. Bethke, U. Lockemann, and K. Puschel, *Quantitative investigations on the human entorhinal area: left-right asymmetry and age-related changes.* Anat Embryol (Berl), 1994. **190**(2): p. 181-94.
3. Glick, S.D., R.A. Lyon, P.A. Hinds, C. Sowek, and M. Titeler, *Correlated asymmetries in striatal D1 and D2 binding: relationship to apomorphine-induced rotation.* Brain Research, 1988. **455**(1): p. 43-48.

4. Pandey, P., M.D. Mersha, and H.S. Dhillon, *A synergistic approach towards understanding the functional significance of dopamine receptor interactions.* J Mol Signal, 2013. **8**(1): p. 13.
5. Navarro, G., S. Ferré, A. Cordomi, E. Moreno, J. Mallol, V. Casadó, A. Cortés, H. Hoffmann, J. Ortiz, E.I. Canela, C. Lluís, L. Pardo, R. Franco, and A.S. Woods, *Interactions between Intracellular Domains as Key Determinants of the Quaternary Structure and Function of Receptor Heteromers.* Journal of Biological Chemistry, 2010. **285**(35): p. 27346-27359.
6. Orru, M., J. Bakešová, M. Brugarolas, C. Quiroz, V. Beaumont, S.R. Goldberg, C. Lluís, A. Cortés, R. Franco, V. Casadó, E.I. Canela, and S. Ferré, *Striatal Pre- and Postsynaptic Profile of Adenosine A_{2A} Receptor Antagonists.* PLoS ONE, 2011. **6**(1): p. e16088.
7. Glick, S.D., D.A. Ross, and L.B. Hough, *Lateral asymmetry of neurotransmitters in human brain.* Brain Research, 1982. **234**(1): p. 53-63.
8. Thiel, C.M. and R.K.W. Schwarting, *Dopaminergic Lateralisation in the Forebrain: Relations to Behavioural Asymmetries and Anxiety in Male Wistar Rats.* Neuropsychobiology, 2001. **43**(3): p. 192-199.
9. Schwarting, R.K.W. and A. Borta, *Analysis of behavioral asymmetries in the elevated plus-maze and in the T-maze.* Journal of Neuroscience Methods, 2005. **141**(2): p. 251-260.
10. Nikkhah, G., G. Falkenstein, and C. Rosenthal, *Restorative Plasticity of Dopamine Neuronal Transplants Depends on the Degree of Hemispheric Dominance.* The Journal of Neuroscience, 2001. **21**(16): p. 6252-6263.
11. Martin-Soelch, C., J. Szczepanik, A. Nugent, K. Barhaghi, D. Rallis, P. Herscovitch, R.E. Carson, and W.C. Drevets, *Lateralization and gender differences in the dopaminergic response to unpredictable reward in the human ventral striatum.* European Journal of Neuroscience, 2011. **33**(9): p. 1706-1715.
12. Larisch, R., W. Meyer, A. Klimke, F. Kehren, H. Vosberg, and H.W. Muller-Gartner, *Left-right asymmetry of striatal dopamine D2 receptors.* Nucl Med Commun, 1998. **19**(8): p. 781-7.
13. Cho, S.S., E.J. Yoon, and S.E. Kim, *Asymmetry of Dopamine D2/3 Receptor Availability in Dorsal Putamen and Body Mass Index in Non-obese Healthy Males.* Exp Neurobiol, 2015. **24**(1): p. 90-94.
14. Tomer, R., H.A. Slagter, B.T. Christian, A.S. Fox, C.R. King, D. Murali, M.A. Gluck, and R.J. Davidson, *Love to Win or Hate to Lose? Asymmetry of Dopamine D2 Receptor Binding Predicts Sensitivity to Reward versus Punishment.* Journal of Cognitive Neuroscience, 2013. **26**(5): p. 1039-1048.
15. Tomer, R., R.Z. Goldstein, G.-J. Wang, C. Wong, and N.D. Volkow, *Incentive motivation is associated with striatal dopamine asymmetry.* Biological Psychology, 2008. **77**(1): p. 98-101.
16. Marin, C., M. Bonastre, G. Mengod, R. Cortés, and M.C. Rodríguez-Oroz, *From unilateral to bilateral parkinsonism: Effects of lateralization on dyskinesias and associated molecular mechanisms.* Neuropharmacology, 2015. **97**: p. 365-375.
17. Farré, D., A. Munoz, E. Moreno, I. Reyes-Resina, J. Canet-Pons, I.G. Dopeso-Reyes, A.J. Rico, C. Lluis, J. Mallol, G. Navarro, E.I. Canela, A. Cortes, J.L. Labandeira-Garcia, V. Casadó, J.L. Lanciego, and R. Franco, *Stronger Dopamine D1 Receptor-Mediated Neurotransmission in Dyskinesia.* Mol Neurobiol, 2014. DOI 10.1007/s12035-014-8936-x

18. Cenci, M.A., C.S. Lee, and A. Björklund, *L-DOPA-induced dyskinesia in the rat is associated with striatal overexpression of prodynorphin- and glutamic acid decarboxylase mRNA.* European Journal of Neuroscience, 1998. **10**(8): p. 2694-2706.
19. Casadó, V., C. Ferrada, J. Bonaventura, E. Gracia, J. Mallol, E.I. Canela, C. Lluís, A. Cortés, and R. Franco, *Useful pharmacological parameters for G-protein-coupled receptor homodimers obtained from competition experiments. Agonist–antagonist binding modulation.* Biochemical Pharmacology, 2009. **78**(12): p. 1456-1463.
20. Casadó, V., A. Cortés, F. Ciruela, J. Mallol, S. Ferré, C. Lluis, E.I. Canela, and R. Franco, *Old and new ways to calculate the affinity of agonists and antagonists interacting with G-protein-coupled monomeric and dimeric receptors: The receptor–dimer cooperativity index.* Pharmacology & Therapeutics, 2007. **116**(3): p. 343-354.
21. Franco, R., V. Casadó, J. Mallol, C. Ferrada, S. Ferré, K. Fuxe, A. Cortés, F. Ciruela, C. Lluis, and E.I. Canela, *The Two-State Dimer Receptor Model: A General Model for Receptor Dimers.* Molecular Pharmacology, 2006. **69**(6): p. 1905-1912.
22. Casadó, V., C. Canti, J. Mallol, E.I. Canela, C. Lluis, and R. Franco, *Solubilization of A1 adenosine receptor from pig brain: characterization and evidence of the role of the cell membrane on the coexistence of high- and low-affinity states.* J Neurosci Res, 1990. **26**(4): p. 461-73.
23. Lee, S.P., C.H. So, A.J. Rashid, G. Varghese, R. Cheng, A.J. Lança, B.F. O'Dowd, and S.R. George, *Dopamine D1 and D2 Receptor Co-activation Generates a Novel Phospholipase C-mediated Calcium Signal.* Journal of Biological Chemistry, 2004. **279**(34): p. 35671-35678.
24. Rashid, A.J., C.H. So, M.M.C. Kong, T. Furtak, M. El-Ghundi, R. Cheng, B.F. O'Dowd, and S.R. George, *D1–D2 dopamine receptor heterooligomers with unique pharmacology are coupled to rapid activation of Gq/11 in the striatum.* Proceedings of the National Academy of Sciences, 2007. **104**(2): p. 654-659.
25. Chun, L.S., R.B. Free, T.B. Doyle, X.-P. Huang, M.L. Rankin, and D.R. Sibley, *D1-D2 Dopamine Receptor Synergy Promotes Calcium Signaling via Multiple Mechanisms.* Molecular Pharmacology, 2013. **84**(2): p. 190-200.
26. Jin, L.-Q., H.-Y. Wang, and E. Friedman, *Stimulated D1 dopamine receptors couple to multiple Gα proteins in different brain regions.* Journal of Neurochemistry, 2001. **78**(5): p. 981-990.
27. Mannoury la Cour, C., S. Vidal, V. Pasteau, D. Cussac, and M.J. Millan, *Dopamine D1 receptor coupling to Gs/olf and Gq in rat striatum and cortex: A scintillation proximity assay (SPA)/antibody-capture characterization of benzazepine agonists.* Neuropharmacology, 2007. **52**(3): p. 1003-1014.
28. May, L.T., L.J. Bridge, L.A. Stoddart, S.J. Briddon, and S.J. Hill, *Allosteric interactions across native adenosine-A3 receptor homodimers: quantification using single-cell ligand-binding kinetics.* The FASEB Journal, 2011. **25**(10): p. 3465-3476.
29. Yamamoto, B.K., R.F. Lane, and C.R. Freed, *Normal rats trained to circle show asymmetric caudate dopamine release.* Life Sci, 1982. **30**(25): p. 2155-62.
30. Cannon, D.M., J.M. Klaver, S.A. Peck, D. Rallis-Voak, K. Erickson, and W.C. Drevets, *Dopamine Type-1 Receptor Binding in Major Depressive Disorder Assessed Using Positron Emission Tomography and [lsqb]11C[rsqb]NNC-112.* Neuropsychopharmacology, 2008. **34**(5): p. 1277-1287.

31. Ryoo, H.L., D. Pierrotti, and J.N. Joyce, *Dopamine D3 receptor is decreased and D2 receptor is elevated in the striatum of Parkinson's disease.* Mov Disord, 1998. **13**(5): p. 788-97.
32. Hurley, M.J., D.C. Mash, and P. Jenner, *Dopamine D1 receptor expression in human basal ganglia and changes in Parkinson's disease1.* Molecular Brain Research, 2001. **87**(2): p. 271-279.
33. Boileau, I., M. Guttman, P. Rusjan, J.R. Adams, S. Houle, J. Tong, O. Hornykiewicz, Y. Furukawa, A.A. Wilson, S. Kapur, and S.J. Kish, *Decreased binding of the D3 dopamine receptor-preferring ligand [11C]-(+)-PHNO in drug-naïve Parkinson's disease*. 132. 2009. 1366-1375.
34. Morin, N., V.A. Jourdain, M. Morissette, L. Grégoire, and T. Di Paolo, *Long-term treatment with l-DOPA and an mGlu5 receptor antagonist prevents changes in brain basal ganglia dopamine receptors, their associated signaling proteins and neuropeptides in parkinsonian monkeys.* Neuropharmacology, 2014. **79**: p. 688-706.
35. Ginés, S., J. Hillion, M. Torvinen, S. Le Crom, V. Casadó, E.I. Canela, S. Rondin, J.Y. Lew, S. Watson, M. Zoli, L.F. Agnati, P. Vernier, C. Lluis, S. Ferré, K. Fuxe, and R. Franco, *Dopamine D1 and adenosine A1 receptors form functionally interacting heteromeric complexes.* Proceedings of the National Academy of Sciences, 2000. **97**(15): p. 8606-8611.
36. Ferre, S., R. Baler, M. Bouvier, M.G. Caron, L.A. Devi, T. Durroux, K. Fuxe, S.R. George, J.A. Javitch, M.J. Lohse, K. Mackie, G. Milligan, K.D.G. Pfleger, J.-P. Pin, N.D. Volkow, M. Waldhoer, A.S. Woods, and R. Franco, *Building a new conceptual framework for receptor heteromers.* Nat Chem Biol, 2009. **5**(3): p. 131-134.
37. El-Asmar, L., J.-Y. Springael, S. Ballet, E.U. Andrieu, G. Vassart, and M. Parmentier, *Evidence for Negative Binding Cooperativity within CCR5-CCR2b Heterodimers.* Molecular Pharmacology, 2005. **67**(2): p. 460-469.
38. Sohy, D., M. Parmentier, and J.-Y. Springael, *Allosteric Transinhibition by Specific Antagonists in CCR2/CXCR4 Heterodimers.* Journal of Biological Chemistry, 2007. **282**(41): p. 30062-30069.
39. Ferré, S., G. Navarro, V. Casadó, A. Cortés, J. Mallol, E.I. Canela, C. Lluís, and R. Franco, *Chapter 2 - G Protein-Coupled Receptor Heteromers as New Targets for Drug Development*, in *Progress in Molecular Biology and Translational Science*, A.L. Charles, Editor. 2010, Academic Press. p. 41-52.
40. Maggio, R., M. Scarselli, M. Capannolo, and M.J. Millan, *Novel dimensions of D3 receptor function: Focus on heterodimerisation, transactivation and allosteric modulation.* European Neuropsychopharmacology, 2015.
41. Borroto-Escuela, D., I. Brito, W. Romero-Fernandez, M. Di Palma, J. Oflijan, K. Skieterska, J. Duchou, K. Van Craenenbroeck, D. Suárez-Boomgaard, A. Rivera, D. Guidolin, L. Agnati, and K. Fuxe, *The G Protein-Coupled Receptor Heterodimer Network (GPCR-HetNet) and Its Hub Components.* International Journal of Molecular Sciences, 2014. **15**(5): p. 8570.
42. Lee, F.J.S., S. Xue, L. Pei, B. Vukusic, N. Chéry, Y. Wang, Y.T. Wang, H.B. Niznik, X.-m. Yu, and F. Liu, *Dual Regulation of NMDA Receptor Functions by Direct Protein-Protein Interactions with the Dopamine D1 Receptor.* Cell, 2002. **111**(2): p. 219-230.
43. Fiorentini, C., F. Gardoni, P. Spano, M. Di Luca, and C. Missale, *Regulation of Dopamine D1 Receptor Trafficking and Desensitization by Oligomerization with*

Glutamate N-Methyl-D-aspartate Receptors. Journal of Biological Chemistry, 2003. **278**(22): p. 20196-20202.
44. Ladepeche, L., L. Yang, D. Bouchet, and L. Groc, *Regulation of Dopamine D1 Receptor Dynamics within the Postsynaptic Density of Hippocampal Glutamate Synapses.* PLoS ONE, 2013. **8**(9): p. e74512.
45. Zheng, Q., Z. Liu, C. Wei, J. Han, Y. Liu, X. Zhang, and W. Ren, *Activation of the D1 receptors inhibits the long-term potentiation in vivo induced by acute morphine administration through a D1-GluN2A interaction in the nucleus accumbens.* Neuroreport, 2014. **25**(15): p. 1191-7.
46. Kisilevsky, A.E., S.J. Mulligan, C. Altier, M.C. Iftinca, D. Varela, C. Tai, L. Chen, S. Hameed, J. Hamid, B.A. MacVicar, and G.W. Zamponi, *D1 Receptors Physically Interact with N-Type Calcium Channels to Regulate Channel Distribution and Dendritic Calcium Entry.* Neuron, 2008. **58**(4): p. 557-570.
47. Koh, P., C. Bergson, A.S. Undie, P.S. Goldman-Rakic, and M.S. Lidow, *UP-regulation of the d1 dopamine receptor–interacting protein, calcyon, in patients with schizophrenia.* Archives of General Psychiatry, 2003. **60**(3): p. 311-319.
48. Lidow, M.S., A. Roberts, L. Zhang, P.-O. Koh, N. Lezcano, and C. Bergson, *Receptor crosstalk protein, calcyon, regulates affinity state of dopamine D1 receptors.* European Journal of Pharmacology, 2001. **427**(3): p. 187-193.
49. Joyce, J.N., N. Lexow, E. Bird, and A. Winokur, *Organization of dopamine D1 and D2 receptors in human striatum: receptor autoradiographic studies in Huntington's disease and schizophrenia.* Synapse, 1988. **2**(5): p. 546-57.

Figure Legends

Figure 1.- Balance of high- and low-affinity states in right and left striatum from different animals groups. The figure has been constructed using data in table 1. In each image the left and weighing plate would correspond to the amount of, respectively, low and high-affinity sites. When the amount of low- is higher than that of high-affinity sites, the left weighing plate is down and the right up; the opposite (left plate up and the right down) occurs when high-affinity sites are more abundant than low-affinity sites. The degree of dysbalance corresponds to the actual differences in the number of high and low-affinity states. The numbers correspond to the affinity values (for each condition) of low (left) and high (right) affinity species.

Figure 2.- Scheme of different protein-protein interactions that may impact on the structure of D_1R and give rise to lateralization of dopamine binding and receptor-mediated signaling. Other G protein-coupled receptors, other membrane proteins, various G proteins and scaffolding proteins may likely interact with dopamine receptors.

Table 1
Click here to download Table: Hints_Table_1_v4.pdf

Table 1. Parameter values for the agonist SKF 38393 obtained using [^{3}H]SCH 23390 as radioligand and data fitting to equations devised from the two-independent site model.

Sample	Side	7-OH-PIPAT (100 nM)	B_{maxH}	K_{DH}	B_{maxL}	K_{DL}	B_{50}
Naïve	right	-	1.1±0.2	28±2	0.85±0.05	410±30	85±20
		+	1.0±0.4	16±3	1.1±0.2	280±50	75±30
	left	-	$0.3\pm0.1^{\#\#\#}$	$2\pm1^{\#\#\#}$	1.4±0.4	$140\pm20^{\#\#\#}$	90±40
		+	0.34±0.07	$5\pm1^{\#}$	1.3±0.4	170±40	105±30
Lesioned	right	-	$0.39\pm0.08^{\&}$	$7\pm3^{\&\&\&}$	1.16±0.08	$220\pm40^{\&\&}$	120±40
		+	$0.38\pm0.05^{\&}$	5±1	1.12±0.05	220±10	115±15
	left	-	0.41±0.05	2±1	1.52±0.05	190±20	115±10
		+	$0.58\pm0.05^{\&}$	7±2	1.30±0.08	240±20	105±30
L-DOPA-treated (non dyskinetic)	right	-	$0.47\pm0.07^{\&}$	$7\pm2^{\&\&\&}$	1.26±0.07	$170\pm20^{\&\&\&}$	90±20
		+	0.8±0.2	$26\pm6^{**}$	1.0±0.2	200±50	80±35
	left	-	0.24±0.05	0.7±0.3	1.73±0.02	120±10	90±10
		+	0.37±0.07	$5\pm2^{\#\#\#}$	1.65±0.07	150±10	100±15
Dyskinetic	right	-	1.2±0.1	24±4	0.9±0.1	420±60	75±20
		+	0.8±0.1	$5\pm2^{**}$	$1.6\pm0.1^{\&**}$	$220\pm20^{**}$	85±20
	left	-	$0.66\pm0.05^{\&\&\#\#}$	$4\pm1^{\#\#\#}$	1.3±0.1	$190\pm20^{\#\#\#}$	70±20
		+	$0.61\pm0.03^{\&}$	3±1	1.24±0.05	190±20	70±10

Data are mean±SEM values from three experiments [see 3]. B_{max} is the maximum specific binding and K_D is the equilibrium dissociation constant of the competing ligand B (SKF 38393). B_{maxH} and B_{maxL} are the maximum specific binding corresponding to, respectively, high- and low-affinity sites, and K_{DH} and K_{DL} are the equilibrium dissociation constants for, respectively, high- and low-affinity sites. B_{50} is the concentration providing half saturation of the receptor for B and is obtained according to Eq. 3.
** p<0,01 comparing with and without treatment with the D_3 receptor agonist, 7-OH-PIPAT. $^{\#}$ p<0,05, $^{\#\#}$ p<0,01 and $^{\#\#\#}$ p<0,001 respect to the right side. $^{\&}$ p<0,05, $^{\&\&}$ p<0,01 and $^{\&\&\&}$ p<0,001 respect to the naïve after Bonferroni's post hoc test.

Table 2
Click here to download Table: Hints_Table_2_v4.pdf

Table 2. Parameter values for the agonist SKF 38393 obtained using [^{3}H]SCH 23390 as radioligand and data fitting to equations devised from the dimer receptor model.

Sample	Side	7-OH-PIPAT (100 nM)	R_T	K_{DB1}	K_{DB2}	D_{CB}	K_{DAB}	D_{AB}	B_{50}
Naïve	right	-	1.0±0.1	22±2	370±40	-0.62	44±4	0	90±9
		+	1.0±0.1	21±6	330±50	-0.59	40±10	0	85±20
	left	-	1.1±0.1	3±1$^{###}$	80±10$^{###}$	-0.82	2±1$^{###}$	0.5	15±4$^{###}$
		+	1.1±0.1	6±2$^{#}$	120±30$^{##}$	-0.70	6±2$^{###}$	0.3	27±8$^{#}$
Lesioned	right	-	0.80±0.03	28±3	450±20	-0.60	56±6	0	112±9
		+	0.75±0.05	22±3	470±40	-0.73	44±6	0	100±10
	left	-	1.0±0.1	3±1$^{###}$	120±20$^{###}$	-1.0	3±1$^{###}$	0.3	19±5$^{###}$
		+	1.0±0.1	7±3$^{#}$	210±40$^{###}$	-0.77	10±4$^{###}$	0.25	40±15$^{##}$
L-DOPA- treated (non-dyskinetic)	right	-	0.9±0.1	20±2	330±30	-0.62	40±4	0	81±8
		+	0.9±0.1	28±2	270±30	-0.38	56±4	0	87±8
	left	-	1.0±0.1	2±1$^{###}$	60±20$^{###}$	-0.88	0.8±0.4$^{###}$	0.7	11±4$^{###}$
		+	1.1±0.1	8±3$^{##}$	90±20$^{##}$	-0.45	7±3$^{###}$	0.35	27±8$^{##}$
Dyskinetic	right	-	1.2±0.1	20±2	340±30	-0.63	40±4	0	82±8
		+	1.2±0.1	5±1$^{\&\&*}$	160±30$^{\&\&**}$	-0.90	6±2$^{\&\&\&**}$	0.2	28±6$^{\&\&}$
	left	-	1.0±0.1	4±1$^{###}$	160±30$^{###}$	-1.0	5±1$^{###}$	0.2	25±5$^{###}$
		+	1.0±0.1	4±1	160±20	-1.0	4±2	0.3	25±5

Data are mean±SEM values from three experiments [see 3]. R_T is the total amount of receptor dimers, K_{DB1} and K_{DB2} are, respectively, the equilibrium dissociation constants of the first and second binding of B to the dimer. K_{DAB} is the hybrid equilibrium dissociation constant of B binding to a receptor dimer semioccupied by the A ([^{3}H]SCH 23390). D_{CB} is the dimer cooperativity index for the binding of ligand B and D_{AB} is the dimer radioligand/competitor modulation index. B_{50} is the concentration providing half saturation for B. Parameters obtained according to [4,5].
* p<0,05 and ** p<0,01 01 comparing with and without treatment with the D_3 receptor agonist, 7-OH-PIPAT. $^{\#}$ p<0,05, $^{\#\#}$ p<0,01 and $^{\#\#\#}$ p<0,001 respect to the right side. $^{\&\&}$ p<0,01 and $^{\&\&\&}$ p<0,001 respect to the naïve after Bonferroni's post hoc test.

Figure 1
Click here to download Figure: Fig_1.tiff

Franco et al., Figure 1

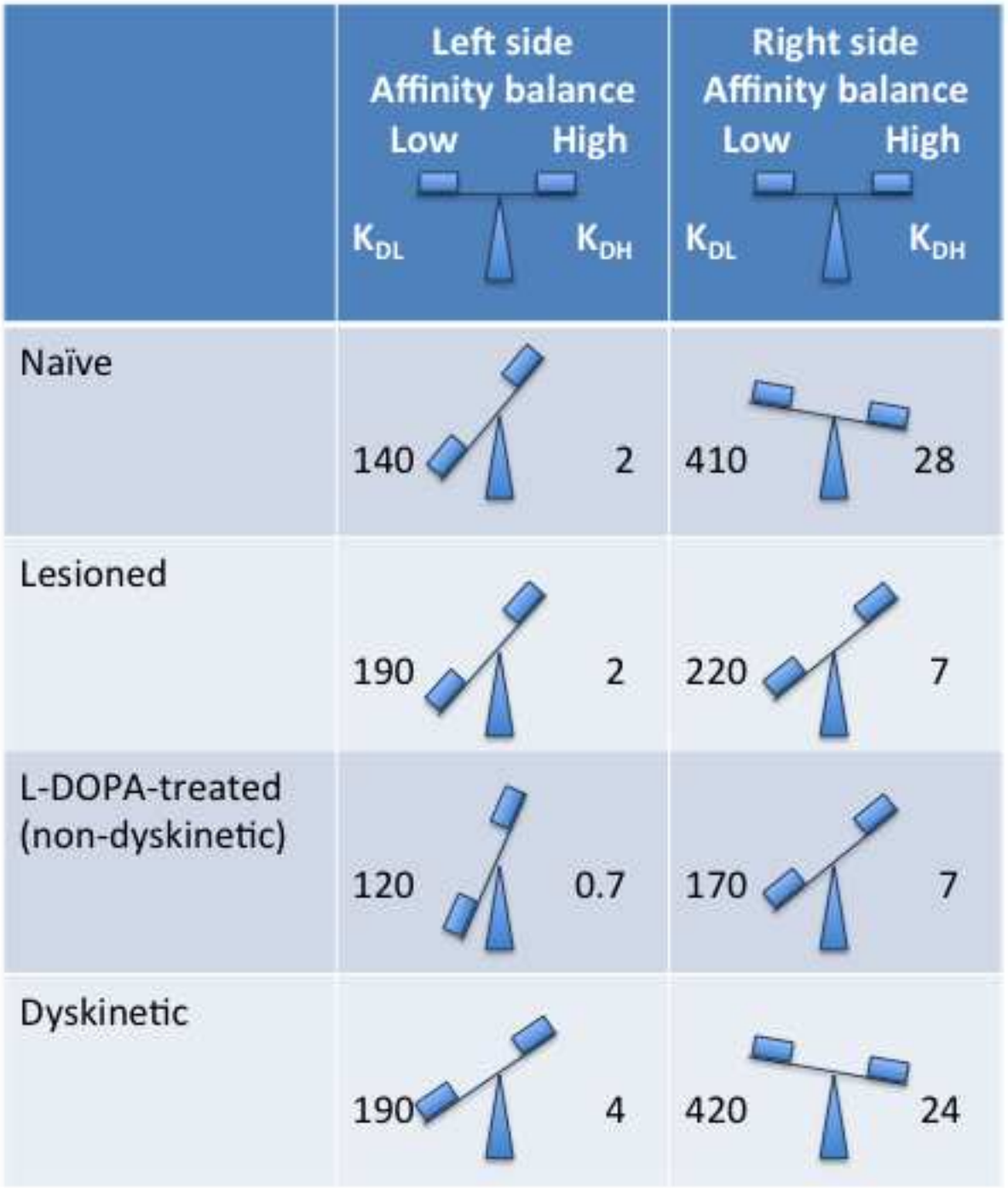

Figure 2
Click here to download Figure: Fig_2.tiff

Franco et al., Figure 2